

This is an Open Access document downloaded from ORCA, Cardiff University's institutional repository:<https://orca.cardiff.ac.uk/id/eprint/133207/>

This is the author's version of a work that was submitted to / accepted for publication.

Citation for final published version:

Church, S. A., Ding, B., Mitchell, P. W., Kappers, M. J., Frentrup, M., Kusch, G., Fairclough, M., Wallis, D. J., Oliver, R. A. and Binks, D. J. 2020. Stacking fault-associated polarised surface-emitted photoluminescence from zincblende InGaN/GaN quantum wells. *Applied Physics Letters* 117 (3), 032103. 10.1063/5.0012131

Publishers page: <https://doi.org/10.1063/5.0012131>

Please note:

Changes made as a result of publishing processes such as copy-editing, formatting and page numbers may not be reflected in this version. For the definitive version of this publication, please refer to the published source. You are advised to consult the publisher's version if you wish to cite this paper.

This version is being made available in accordance with publisher policies. See <http://orca.cf.ac.uk/policies.html> for usage policies. Copyright and moral rights for publications made available in ORCA are retained by the copyright holders.



Stacking fault-associated polarised surface-emitted photoluminescence from zincblende InGaN/GaN quantum wells

S. A. Church,¹ B. Ding,² P. W. Mitchell,¹ M. J. Kappers,² M. Frentrup,² G. Kutsch,² S. Fairclough,² D. J. Wallis,^{2,3} R. A. Oliver,² and D. J. Binks¹

¹*Department of Physics and Astronomy, Photon Science Institute, University of Manchester, Manchester M13 9PL, United Kingdom*

²*Department of Materials Science and Metallurgy, University of Cambridge, 27 Charles Babbage Road, Cambridge CB3 0FS, United Kingdom*

³*Centre for High Frequency Engineering, University of Cardiff, 5 The Parade, Newport Road, Cardiff, CF24 3AA, United Kingdom*

S1. SUPPLEMENTARY MATERIAL

A. Photoluminescence results

Fig. S1 shows the PL spectra measured at 10 K for samples with QW widths of 2 nm, 4 nm, 6 nm and 8 nm. In each spectrum the two emission peaks are observed, corresponding to emission from the indium-rich regions of the QWs at low energy (Qwires), and the rest of the QWs at higher energy. There is no trend in the integrated intensity of the emission with QW widths.

The temperature dependence of the PL spectrum was measured for the 2 nm QW sample: these spectra are shown in Fig. S2(a). At low temperatures, the emission peaks from the two recombination mechanisms are both distinct. As the temperature increases up to 100 K the intensity of the emission increases by 10%. This change is small, and occurs across the whole spectrum, and is therefore not associated with the redistribution of carriers amongst the radiative states. This may be associated with an increase in the carrier capture cross section into the QWs with increasing temperature. As the temperature is increased further, the intensity of the higher energy peak, associated with emission from the QWs, re-

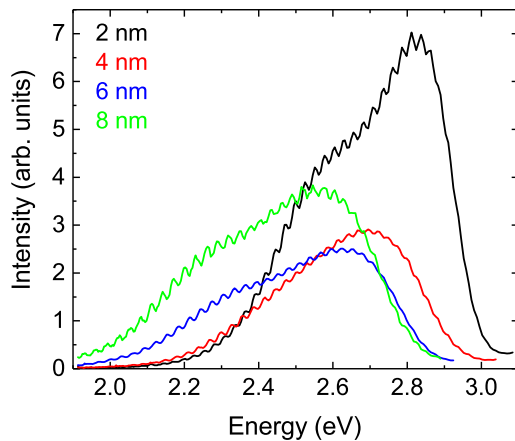


FIG. S1. The 10 K PL spectra of zb-InGaN/GaN QW samples with QW thicknesses of 2 nm, 4 nm, 6 nm and 8 nm.

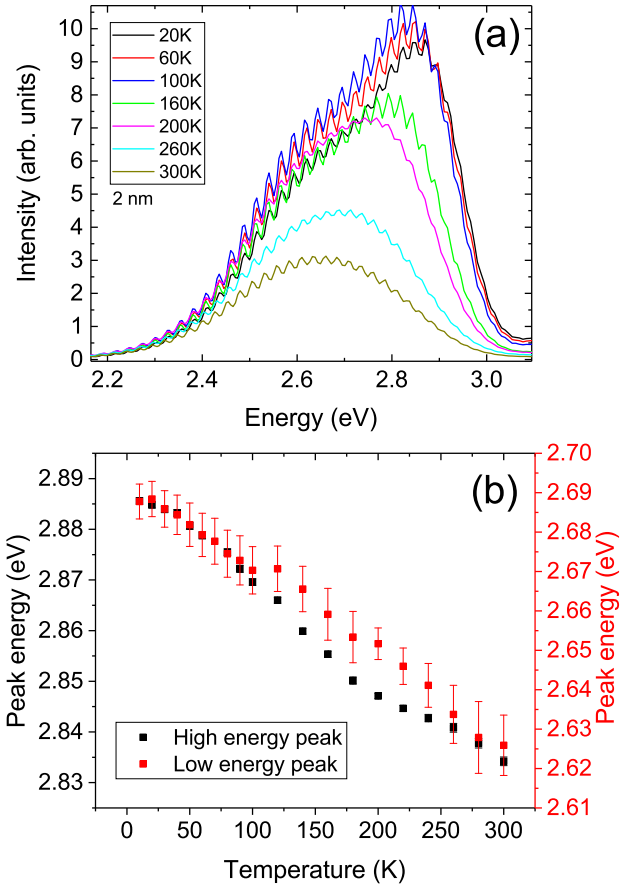


FIG. S2. PL spectra of the 2 nm (a) QW sample using a CW HeCd laser with an excitation power density of 10 W cm^{-2} , at different temperatures. (b) Peak energies of the high energy and low energy peak at each temperature, extracted using a bi-Gaussian fit.

duces faster with increasing temperature than the Qwire associated peak. Once the temperature is above 260 K, only the Qwire peak remains in the spectrum. The peak energy of the high and low energy peaks was extracted using a bi-Gaussian fit, as shown in Fig. S2(b). Both peaks redshift by 70 meV, which is broadly uniform over the temperature range.

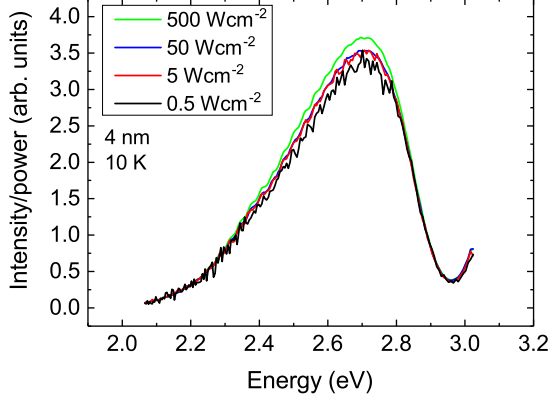


FIG. S3. 10 K The PL spectra of the 4 nm QW sample using a CW HeCd laser with different excitation power densities. Intensity/power is plotted, which gives a measure of the relative efficiency of the recombination between each spectra.

A key indicator of carrier localisation is an observed "s-shape" in the temperature dependence of the peak emission energy¹. There is no evidence of these phenomena in these spectra and the peak emission energy redshifts with increasing temperature. This may mean that localisation of carriers does not play a significant role in recombination in these samples. Alternatively, the localisation phenomena may be obscured by the large FWHM of the peaks, as well as the large spectral overlap of the two emission peaks and the Fabry-Perot interference.

The power dependence of the PL spectrum was investigated using a CW HeCd laser at a wavelength of 325 nm. The excitation power density was varied between 0.5 W cm^{-2} and 500 W cm^{-2} at a temperature of 10 K for the 4 nm-wide QW sample: the resulting PL spectra are shown in Fig. S3.

The integrated intensity of the emission divided by the excitation power increases by only 10% over a three orders of magnitude change in the excitation power density. This suggests that the recombination efficiency is similar at all excitation powers studied. The spectral shape, peak energy and FWHM are unaffected by the excitation power density in this regime: demonstrating that band filling due to photogenerated carriers is negligible in these samples.

Additional PLE measurements were performed using a polarised excitation source, using a CW dye laser. The polarisation was controlled using a Fresnel Rhomb to rotate the polarisation direction. The excitation wavelength was varied between 416 nm and 465 nm. The excitation power density was measured to be around 1.4 kW cm^{-2} for all wavelengths, and the unpolarised emission spectra were normalised to the power at each wavelength. The experiment was performed for the 6 nm wide QW sample and the results are shown in Fig. S4.

When exciting the QWs directly, with a wavelength of 416 nm, the PL spectrum and the intensity of the emis-

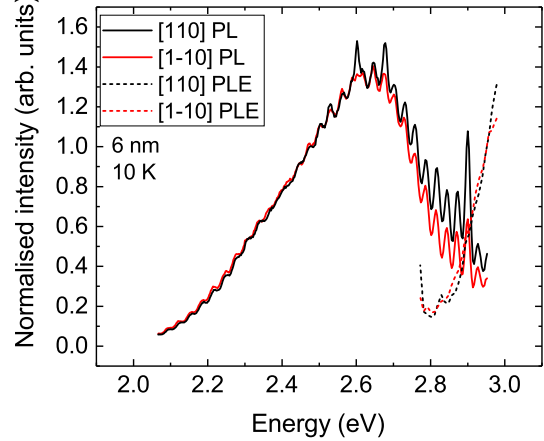


FIG. S4. 10 K PL (solid) and PLE (dashed) measurements of the 6 nm QW sample using a polarised excitation source. The excitation wavelength for the PL spectrum shown was 416 nm and the PLE was measured at an emission wavelength of 472 nm. The polarisation direction of the source was rotated from [110] (black) to [1-10] (red) using a Fresnel Rhomb.

sion are not affected by the polarisation of the excitation source. This is compatible with the model of the polarised recombination originating from Qwires within the QWs. The majority of absorption will occur in the QW states, where the absorption does not depend on the polarisation. Carriers will then cool and be captured by the polarised Qwire states, and recombine to produce polarised light. The polarised PLE results in Fig. S4 also demonstrate this behaviour, showing no difference in intensity over the excitation wavelength range possible in the experiment.

In heterostructures where the electric field is reduced, recombination may involve excitons². In the absence of localisation effects, the radiative lifetime is still dependent upon the QW-width due to changes in the exciton binding energy, but such effects are small³. Another possibility is that the recombination involves holes and an excess of electrons. In this case the abundance of electrons would limit the variation in the electron-hole wavefunction overlap with QW width. It is challenging to distinguish between these situations because any slight variation in the decay times may be obscured by the disorder in the QWs, which is evidenced in Fig. 4, and therefore a random variation in the decay time is observed.

Additionally, the decay shape is monoexponential, as shown in Fig. 3. This decay shape is consistent with excitonic recombination². However, the same decay shape can result from there being an excess of electrons in the structure⁴.

At the lowest energies there is also no obvious trend in the decay times, which are 375 ps, 365 ps, 330 ps and 410 ps with increasing QW width. The recombination lifetime of the lower energy peak therefore also does not

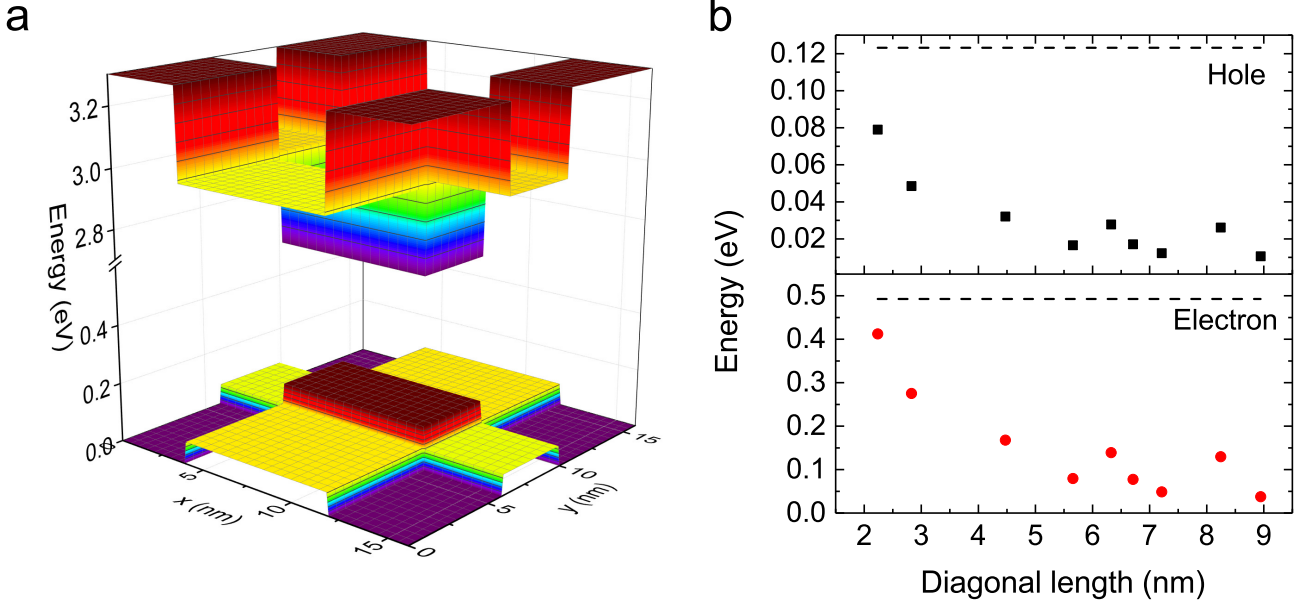


FIG. S5. An example of the conduction band minima and valence band maxima used for the model, describing two intersecting QWs, with widths of 4 nm and 6 nm, each with an indium content of 0.2 (a). This creates a quantum wire with a rectangular profile and an indium content of 0.4. The potentials are assumed to be constant in the third dimension. The calculated ground state energies of electrons and holes, relative to the bottom of the quantum wire, for different quantum wire cross-sectional dimensions and the same indium content as Fig. S5a (b). The dotted line is the energy of the bottom of the QW, i.e. the energy required for the carriers to escape the quantum wire.

vary significantly with QW width, despite the influence of the SFs creating electric fields in these regions. However, these electric fields are not transverse to the QW, instead in the four possible [111] directions, meaning that the QW width will have little effect on the carrier separation by these fields and therefore minimal effect on the decay times. The distance separating the SFs will instead determine the electric fields and hence the decay times⁵.

B. Modelling of quantum wires

To determine if carriers can be captured by the regions of high indium content a three-dimensional model system was developed, as shown in Fig. S5a. This system consisted of two intersecting QWs with the same indium content forming a rectangular cross-sectioned quantum wire with double the indium content where they intersect. The dimensions of the QWs were varied, along with the indium content, calculating the ground state energies for electrons and holes using the Numerov method⁶, the Coulomb effect was accounted for in a similar manner to previous work⁵. Using this model system allowed the Schrödinger equation to be solved separately in each dimension, greatly reducing the complexity of the problem. Parameters used in the modelling are provided in Table S1. In the following analysis, the calculated pa-

	E_g (eV)	m_h^* (m_0)	m_e^* (m_0)	ϵ
GaN	3.30	2	0.2	9.7^7
InN	0.78	2	0.2	9.7^7

TABLE S1. Parameters used for the modelling of quantum wires. Unless specified, parameters have been taken from ref⁸. The bowing parameter for wz-InGaN was used to calculate the bandgap, which was taken to be 1.4. It was assumed that at the QW interfaces the valence band is offset by 20% of the bandgap difference.

rameters are plotted against the length of the diagonal in the cross-section of the quantum wire.

Fig. S5b shows the calculated ground state energies of electrons and holes relative to the bottom of the quantum wire, for different dimensions of the quantum wire, with an indium content of 0.2 in the QWs (and 0.4 in the quantum wire (QWire)). Both holes and electrons are confined to the QWire and this degree of confinement increases with increasing indium composition and QW width. In most cases, the energy required for the carriers to escape the QWire into the QW is much greater than the average thermal energy at room temperature (26 meV). Therefore it is possible for these QWires to trap both electrons and holes.

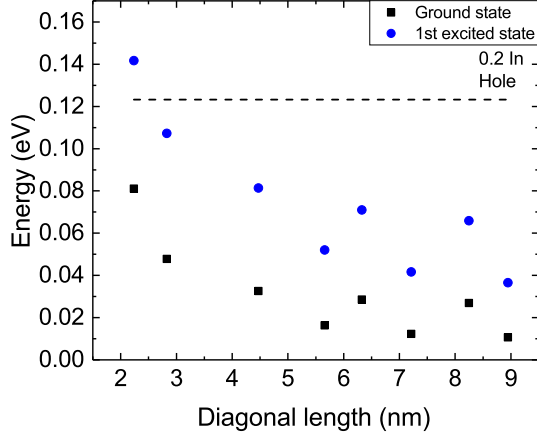


FIG. S6. The calculated heavy hole ground state energies and estimated 1st excited state energies for quantum wire systems with different dimensions and an indium content of 0.2 in the QW. The dotted line is the energy of the bottom of the QW, i.e. the energy required for the carriers to escape the quantum wire.

According to Bockelmann and Bastard⁹, mixing of heavy and light holes in the QWire will result in the emission of light polarised in different directions. Electron-hole ground state recombination will emit light polarised along the QWire. At low temperatures and low carrier densities, only the ground states will be occupied, and therefore the overall emission from the QWires will be polarised. This is consistent with PL measurements in Fig. 2, where the DOLP of the QWire emission at 10 K is 86 %. The DOLP will depend upon the cross sectional area of the QWires: narrower QWires will have a higher DOLP¹⁰.

Higher order states confined to the QWire can emit light polarised orthogonally to the ground state⁹, therefore the DOLP of the emission will drop if the higher order states are populated, which may occur at elevated temperatures. Measurements shown in Fig. 1 demonstrate that the DOLP of the QWire emission at 300 K is as high as 75 %, a drop of roughly 10 % from low temperature measurements. The DOLP can be independent of temperature if there are no excited states in the QWire, or may weakly depend on the temperature if the splitting between the ground and excited states is large compared with the average thermal energy (kT). The energy of these excited states will depend upon the dimensions of the QWires¹⁰. To estimate the energy of these excited states, the ground state energies for light holes (taken to have a mass of $0.2m_0$) were calculated as the upper limit for these excited states. A slightly improved estimate of the splitting was obtained by halving the separation of the heavy and light hole states, as the excited states lie between these two⁹. The parameters of the system were varied to estimate how this splitting

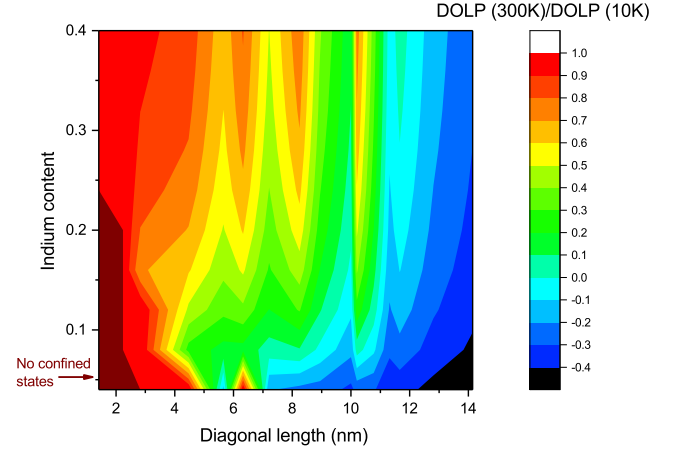


FIG. S7. Calculated ratio of the DOLP at 300 K and 10 K, taking into account the thermal equilibrium population of the ground and excited states, assuming the recombination rate is unaffected. For indium contents below 0.25 and diagonal lengths of less than 2 nm there are no confined states.

depends on the indium content and the dimensions of the QWire, the results for an indium content of 0.20 are shown in Fig. S6.

For the narrowest dimensions calculated, the excited state lies above the barrier and therefore is not confined to the QWire. In this case, the DOLP will be independent of temperature. As the dimensions of the wire are increased, the splitting reduces from 60 meV to 26 meV. Therefore, at room temperature, the excited state will be populated to a greater extent for wider quantum wires and the DOLP of the emission from wider wires will decrease more as the temperature is increased.

Assuming that a thermal equilibrium is reached during the experiment, this dependence was estimated by calculating the relative occupation of the ground state and 1st excited state at room temperature using Boltzmann statistics. The ratio of the DOLP at 300 K and 10 K was then estimated for different indium contents and dimensions, by assuming that the recombination rate of each state is identical: the results are shown in Fig. S7.

It is possible to achieve a change in the DOLP which is less than 10 % by using quantum wires with a diagonal cross sectional length less than 3 nm. Therefore, this simple model suggests that achieving a small change in the DOLP between 10 K room temperature is feasible.

In general, narrower quantum wires and higher indium contents will make the DOLP less dependent upon temperature. The "jagged" nature of this plot is due to separate changes in the two dimensions of the cross section, whilst the data is plotted only against the quadrature sum of these: if one dimension is significantly narrower than the other this results in an increase in the calculated ratio.

Blue colours in Fig. S7 demonstrate that the polari-

sation is expected to be in the orthogonal direction at room temperature for diagonal lengths above 7 nm for low indium contents, and above 11 nm for high indium contents. However, such an effect is unlikely to be observed since the DOLP will reduce to zero with increasing dimensions⁹.

This work was funded by EPSRC under grants EP/M010627/1, EP/N01202X/1 and EP/R01146X/1, and Innovate UK under grant 56917-383420. The authors would like to thank Prof. Phil Dawson (University of Manchester) for useful discussions.

DATA AVAILABILITY

Research data supporting this publication are available at DOI: 10.17632/74x2spfrk2.1.

- ¹O. Rubel, M. Galluppi, S. D. Baranovskii, K. Volz, L. Geelhaar, H. Riechert, P. Thomas, and W. Stolz, *J. Appl. Phys.* **98**, 063518 (2005).
- ²P. Dawson, S. Schulz, R. A. Oliver, M. J. Kappers, and C. J. Humphreys, *J. Appl. Phys.* **119**, 181505 (2016).
- ³J. Feldmann, G. Peter, E. O. Göbel, P. Dawson, K. Moore, C. Foxon, and R. J. Elliott, *Phys. Rev. Lett.* **59**, 2337 (1987).
- ⁴H. Haratizadeh, B. Monemar, P. P. Paskov, P. O. Holtz, G. Pozina, S. Kamiyama, M. Iwaya, H. Amano, and I. Akasaki, *Phys. status solidi* **241**, 1124 (2004).
- ⁵S. A. Church, S. Hammersley, P. W. Mitchell, M. J. Kappers, L. Y. Lee, F. Massabuau, S. L. Sahonta, M. Frentrup, L. J. Shaw, D. J. Wallis, C. J. Humphreys, R. A. Oliver, D. J. Binks, and P. Dawson, *J. Appl. Phys.* **123**, 185705 (2018).
- ⁶A. C. Allison, *J. Comput. Phys.* **6**, 378 (1970).
- ⁷V. Bougrov, M. E. Levinshtein, S. L. Rumyantsev, and A. Zubrilov, *Properties of Advanced Semiconductor Materials GaN, AlN, InN, BN, SiC, SiGe* (John Wiley & Sons, 2001) pp. 1–30.
- ⁸I. Vurgaftman and J. R. Meyer, *J. Appl. Phys.* **94**, 3675 (2003).
- ⁹U. Bockelmann and G. Bastard, *Phys. Rev. B* **45**, 1688 (1992).
- ¹⁰W. H. Zheng, J.-b. Xia, and K. W. Cheah, *J. Phys. Condens. Matter* **9**, 5105 (1997).